ELSEVIER

Polymer 43 (2002) 4385–4390

polymer

www.elsevier.com/locate/polymer

Aggregation in Langmuir and Langmuir–Blodgett films of azopolymers and its role for optically induced birefringence

D.S. Dos Santos Jr., C.R. Mendonça, D.T. Balogh*, A. Dhanabalan, J.A. Giacometti, S.C. Zilio, O.N. Oliveira Jr.

Instituto de Física de São Carlos, Universidade de São Paulo, Caixa Postal 369, CEP 13560 970, São Carlos, SP, Brazil

Received 19 December 2001; received in revised form 15 April 2002; accepted 17 April 2002

Abstract

Aggregation in azopolymers is reported to affect the Langmuir monolayer characteristics and the optically induced birefringence of Langmuir–Blodgett (LB) films from DR19 isophorone polyurethane (PIPDI) and DR19 4,4′ diphenylmethane polyurethane (PMDI). In mixed monolayers with cadmium stearate (CdSt), the folding of PMDI molecules appears to be substantially changed compared to the monolayer of the pure polymer, leading to a surface potential that is higher than observed for monolayers of pure PMDI and of pure CdSt. UV–Vis spectroscopy data of the deposited mixed LB films indicate H-type aggregation for PMDI/CdSt, in contrast to PIPDI/CdSt and other azopolymers investigated earlier. The H-type aggregation precludes photoisomerization, thus requiring a higher laser power for the maximum induced birefringence to be achieved in LB films of PMDI/CdSt.

Keywords: Langmuir–Blodgett; Optical storage; Azopolymer

1. Introduction

A number of molecular engineering strategies have been used to optimize the photoisomerization properties of thin films of azonbezene-containing materials [1]. Photoisomerization is responsible for various interesting phenomena, such as induced birefringence exploited in optical switching [2] and optical modulators [3], and photoinduced mass transport [4] exploited in holography [4–6] and command surfaces for controlling the alignment of liquid crystals and optical storage [7]. The dynamics of the induced birefringence, the maximum values it achieves and the remnant value after the writing laser is switched off depends on a number of characteristics of the polymeric system and on experimental conditions [8,9]. These include the polymer structure and its glass transition temperature (T_g), the nature of the azobenzene chromophore attached to the polymer backbone, the amount of chromophore in the material, the wavelength and power of the laser employed to induce the birefringence [9]. Of particular relevance is the aggregation of chromophores, which may hamper photoisomerization completely. This was the case of Langmuir–Blodgett (LB) films of stearates containing an azochromophore in the headgroup [10], in which the close packing of the LB film impaired photoisomerization. It should be stressed, however, that photoisomerization is still possible and very efficient in LB films but formed with azobenzene-containing polymers [11], especially because the molecular design may be aimed at preventing aggregation.

In this paper we shall discuss the role of chromophore aggregation in LB films from two types of polyurethane polymer, viz. DR19 isophorone polyurethane (PIPDI) and DR19 4,4′ diphenylmethane polyurethane (PMDI), shown in Fig. 1. The use of the LB technique is motivated by the precise thickness control and larger birefringence's owing to the organized nature of the films. Since Langmuir monolayers from azopolymers are poorly transferable, optical-quality LB films with a large number of layers were obtained with the mixed monolayer approach [11]. In this approach, the polymer is cospread with a good film-forming material. It will be shown that already at the air/water interface, aggregation of chromophores affects the properties of the Langmuir film.

2. Experimental part

The synthesis and characterization of PIPDI and PMDI

* Corresponding author. Tel.: +55-16-2739825; fax: +55-16-2715365.
E-mail address: balogh@if.sc.usp.br (D.T. Balogh).

0032-3861/02/$ - see front matter
PII: S0032-3861(02)00279-3

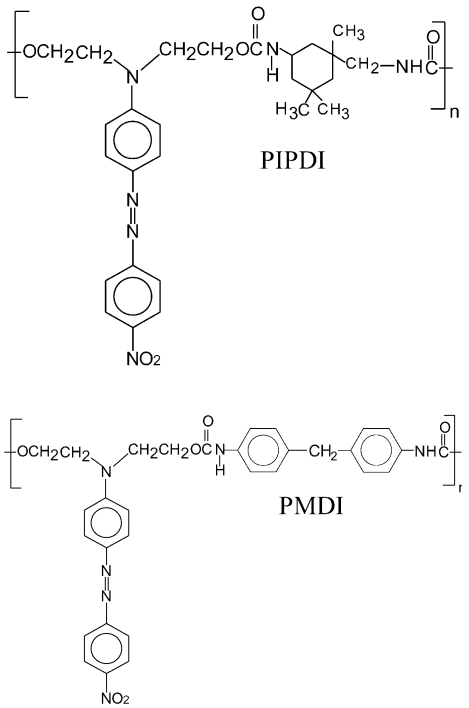

Fig. 1. Structure of PIPDI and PMDI.

were described in Refs. [12,13]. Monolayer experiments and LB depositions were carried out at a subphase temperature of 22 °C with a KSV-5000 LB system housed in a class 10,000 clean room. Ultrapure water supplied by a Milli-RO coupled to a Milli-Q purification system was used to prepare subphase solutions. Monolayers were obtained by spreading a solution of the polymer in a mixture of chloroform–dimethylsulfoxide (8:2 ratio) on a pure water surface. Initial attempts to use chloroform as the spreading solvent resulted in unstable solutions. For the composite monolayers with cadmium stearate (CdSt), a solution with 50%/50% by weight of PIPDI or PMDI and stearic acid in a chloroform–dimethylsulfoxide mixture was spread on an aqueous subphase containing 4×10^{-4} M cadmium chloride and 5×10^{-5} M sodium bicarbonate whose pH was approximately 6.0. During the isotherm experiments, monolayers were compressed at a barrier speed of 10 mm/min. In the case of pure polymers, the monomer repeat unit was considered for mean molecular area (mma) calculations. For the composite monolayers, mma was calculated per stearic acid molecule. BK7 glass slides were cleaned using the RCA method [14] prior to use. UV–Vis measurements were carried out with a Hitachi-U2001 spectrophotometer.

The optical birefringence was induced in the LB film using a polarized Nd/YAG continuous laser at 532 nm with a polarization angle of 45° with respect to the polarization orientation of the probe beam. The power of the writing laser beam was varied up to 12 mW for a 2 mm spot. A low power He–Ne laser at 632.8 nm passing through crossed

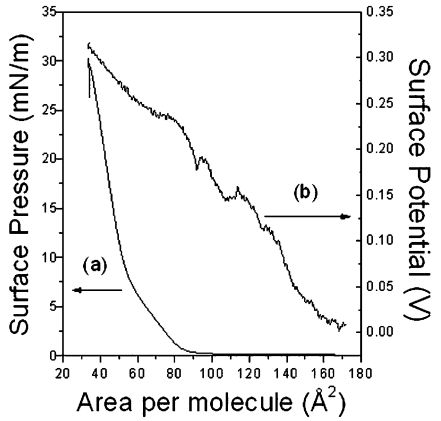

Fig. 2. Surface pressure (curve-a) and surface potential (curve-b) isotherms of a PIPDI monolayer. The abscissa brings the area per monomer.

polarizers was used as the probe beam (reading light) to measure the induced birefringence in the sample.

3. Results and discussion

The surface pressure isotherm for a pure monolayer of PIPDI is shown in curve (a) in Fig. 2, featuring a liftoff area of 90 Å^2 per monomer, and a liquid-expanded region up to 8 mN/m at 55 Å^2. Upon further compression, the pressure increases more steeply up to 28 mN/m, followed by collapse indicated by a slight change in the isotherm slope. The extrapolated area to zero pressure for the most condensed region is 60 Å^2. For the pure PMDI monolayer, curve (a) in Fig. 3 shows a lower liftoff area of 50 Å^2, with a less defined liquid-expanded region in comparison to PIPDI. The extrapolated area for the condensed region is ca. 45 Å^2 and collapse at approximately 28 mN/m, where the latter was determined by taking the derivative of the area in relation to the pressure in the pressure region between 15 and 30 mN/m. PIPDI appears to have a higher affinity for

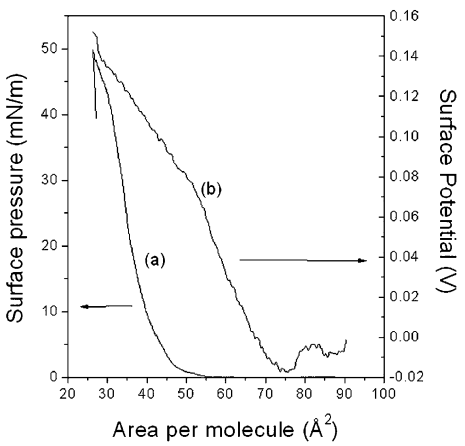

Fig. 3. Surface pressure (curve-a) and surface potential (curve-b) isotherms of a PMDI monolayer. The abscissa brings the area per monomer.

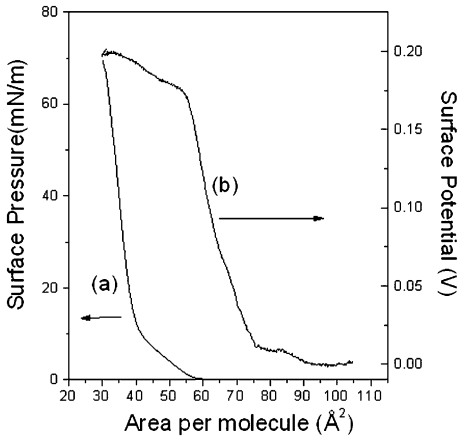

Fig. 4. Surface pressure (curve-a) and surface potential (curve-b) isotherms of a composite monolayer of PIPDI and CdSt (50%:50%). The area is per stearic acid molecule.

water, as its minimum area is larger than PMDI, even though its repeating unit should occupy a smaller area than the PMDI monomer (see the structures in Fig. 1). It should be stressed that current experimental techniques for characterization of Langmuir monolayers do not allow for the determination of the structure adopted by macromolecules at the air/water interface. Nevertheless, the pressure–area isotherms may be used to make inferences as to the possible folding of distinct polymer molecules that are compared directly. Accordingly, the areas per molecule extracted from our pressure–area isotherms indicate that the PIPDI macromolecules are probably less folded than those of PMDI, which could be attributed to the higher attraction of PIPDI to the water.

The pressure and surface potential isotherms for the mixed monolayers with CdSt are shown in Figs. 4 and 5 for PIPDI and PMDI (50%:50% in mass), respectively. The abscissa brings the area per molecule of stearic acid. The liftoff area for both types of film was approximately 55 Å^2 per stearic acid molecule, thus indicating the presence of the polymer at the interface. The collapse pressures for the monolayers were also similar for the two mixed films, being higher than for the pure polymers owing to the presence of

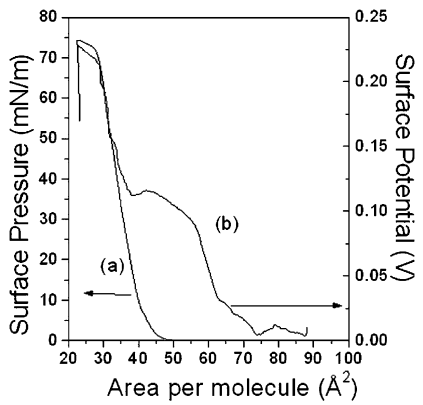

Fig. 5. Surface pressure (curve-a) and surface potential (curve-b) isotherms of a composite monolayer of PMDI and CdSt (50%:50%).

CdSt. The main difference between the two systems is the less well-defined liquid-expanded region for PMDI/CdSt, analogous to what was observed with the monolayer of the pure polymer. The extrapolated areas for the two systems are now very close, which means that the molecular arrangement of the polymer was affected by CdSt, since in the pure monolayers PMDI occupied a smaller area.

Surface potential isotherms were also obtained for the monolayers investigated. The data cannot be treated quantitatively, for it is not possible to estimate the dipole moment contributions from the macromolecules. The surface potential isotherms are nevertheless useful for three reasons: (i) any abrupt molecular reorientation during monolayer compression should lead to significant changes in the surface potential; (ii) the formation of aggregates at large areas per molecule causes the surface potential to be non-zero and irreproducible when distinct monolayers spread under identical conditions are analyzed; (iii) a comparison of isotherms of similar systems may provide information on aggregation and importance of functional groups with large dipole moments [1]. For the polymers investigated here, the differences in folding and aggregation of the macromolecules were also reflected in the surface potential measurements. The monolayer of pure PIPDI displayed a maximum surface potential of 300 mV, while the mixed one with CdSt had a maximum potential of ca. 200 mV, as shown in Figs. 2 and 4, respectively. As expected, the potential for the mixed film is intermediate between the values of the pure polymer and CdSt (120 mV [15]). For PMDI, on the other hand, an unusual behavior was observed, for the maximum potential values of the pure polymer and mixed monolayer were 150 and 250 mV, respectively (Figs. 3 and 5). That is to say, the potential for the mixed monolayer is higher than for either the pure components, which is possible only if strong interaction occurs between the polymer and CdSt.

As observed in the pressure–area isotherms, the area for PMDI was lower than for PIPDI in the pure monolayers, because PMDI was more folded or aggregated, while for the mixed monolayers the areas were essentially the same. Therefore, in the mixed films the folding and/or aggregation of one or the two polymers were affected. Considering the surface potential data, it is more likely that the folding of PMDI was substantially changed, causing its dipolar contribution to increase in the mixed monolayer as compared to the pure one. Indeed, a less folded or aggregated arrangement of PMDI should lead to a larger contribution to the vertical dipole moment (that ultimately defines the surface potential), owing to a lesser degree of canceling of the dipole moments present in the macromolecules. In summary, the surface pressure and surface potential results indicate that CdSt affects strongly the molecular arrangement of PMDI, but apparently not of PIPDI. This also points to distinct aggregation characteristics for the two polymers, which is confirmed in the LB film characterization discussed later.

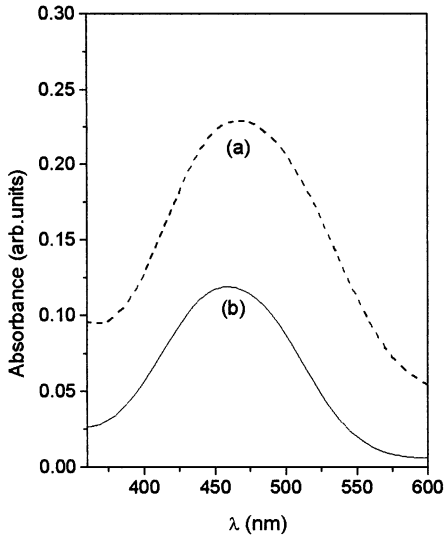

Fig. 6. UV–Vis spectra of PIPDI/CdSt solution (curve-a) and LB film (curve-b).

The deposition of LB films of pure PIPDI and PMDI at a fixed surface pressure of 15 mN/m resulted in low transfer ratios and visually non-uniform films. We therefore resorted to the cospreading method, by mixing each of the polymers with stearic acid and spreading the solution on a cadmium-containing subphase. Mixed LB films of polymer and CdSt could be obtained, where deposition was carried out at a surface pressure of 31 mN/m, with TR of approximately 1 for upstrokes as well as downstrokes (Y-type LB films). The UV–Vis spectra of LB mixed films of PIPDI/CdSt (Fig. 6) show a red shift of approximately 10 nm (maximum at 460 nm) when compared to the polymer in solution (maximum at 470 nm), probably due to J-type aggregation [12]. The LB films, on the other hand, displayed a blue shift of 5 nm, which is characteristic of H-type aggregation. The UV–Vis spectra of PMDI/CdSt, can be found in Ref. [13]. Other related LB films investigated in our group, viz. HPDR13 (poly[4′-[[2-(methacryloyloxy)-ethyl]ethylamino]-2-chloro-4-nitroazobenzene) and copolymers with HEMA (hydroxyethyl-methacrylate), also displayed J-aggregation, whereas the copolymer with only 6% of the dye did not show any shift since aggregation was prevented by the large number of spacers between chromophores [16,17]. Note that only the PMDI/CdSt displayed a blue shift, i.e. H-type aggregation, which makes it distinct from the other systems. This is probably the reason why its interaction with CdSt causes the surface potential of the mixed film to be higher than for both pure components.

Phase separation in the mixed LB films was investigated using X-ray diffraction. Fig. 7 shows for a 21-layer LB film of PMDI/CdSt Bragg peaks characteristic of CdSt domains, with a bilayer distance of approximately 50 Å. Similar results were found for PIPDI/CdSt [12]. This is typical of polymeric mixed LB films where CdSt and the polymer are present in separate domains [15]. Therefore, the strong interaction between PMDI and CdSt seemed only to have

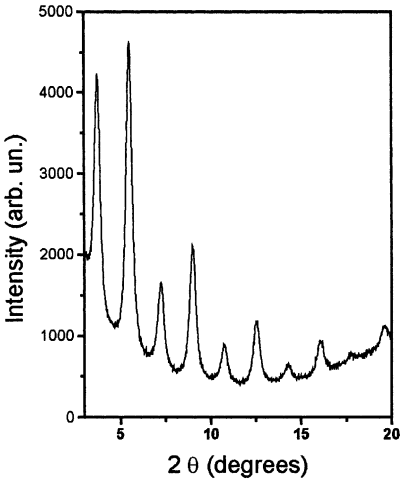

Fig. 7. X-ray diffraction pattern of a mixed 21-layer LB film of PMDI/CdSt.

affected the polymer, as the CdSt domains detected in X-ray diffraction display the same properties as in the PIPDI system.

The optically induced birefringence was investigated in various films: mixed LB films of polyurethanes (PMDI and PIPDI) and CdSt (50%/50%, w/w), and spin-coated films of the pure polymers. Fig. 8 shows the process of writing information in PMDI/CdSt and PIPDI/CdSt 61-layer LB films with the writing laser operating at saturation power. The maximum induced birefringence for the two systems is shown in Table 1. Δn was obtained from

$$\Delta n = \sqrt{T\frac{\lambda}{\pi D}},$$

where T is the transmission after the second polarizer, λ is the wavelength of the reading beam and D is the LB film thickness, estimated using 20 Å per layer. It is clear that the maximum birefringence in LB films is higher for PMDI/CdSt. The time to achieve 50% of the maximum induced birefringence, $T_{50\%}^{\text{write}}$, is about three times slower for PMDI/CdSt than for the PIPDI/CdSt sample. The residual signal and the relaxation time, $T_{50\%}^{\text{relax}}$, are also slightly higher for the PMDI/CdSt sample. Since the structural characteristics

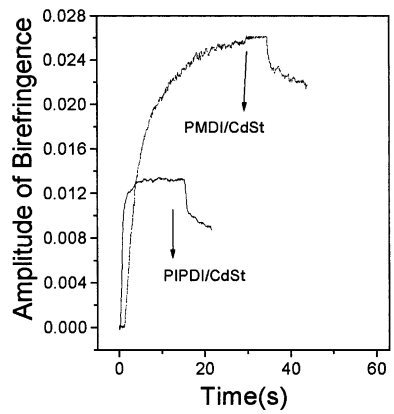

Fig. 8. Birefringence as a function of time for mixed LB films of PIPDI/CdSt (layer) and PMDI/CdSt (61-layer).

Table 1
Characteristics of the induced birefringence for mixed LB films of PIPDI and PMDI

	Maximum Δn	$T_{50\%}^{write}$ (s)	Remnant signal	$T_{50\%}^{relax}$ (s)	Amount of chromophore (% m/m)
PIPDI/CdSt	0.013	0.8	0.70	0.6	59
PMDI/CdSt	0.026	2.8	0.80	0.9	56

(T_g and amount of chromophore) of both polymers are similar, the differences in the optical storage features should be attributed to the different types of aggregation in the LB films. The distinct aggregation of MDI/CdSt may preclude molecular reorientation, thus leading to slower writing and relaxation processes. As a consequence of this lower chromophore mobility, once the molecules have been oriented they will tend to maintain their position. The residual signal and the maximum induced birefringence should then be higher, as observed experimentally. No attempt was made to test the fatigue of the writing–erasing process, but repeating the experiment for more than 10 writing–erasing cycles lead to the same results [17]. Note also that identical optical storage results were obtained if different points of the LB films were taken, thus indicating the homogeneity of the films in terms of the optical properties.

Fig. 9 shows that the maximum induced birefringence increases with the power of the writing laser in a 61-layer LB film of PIPDI/CdSt (50–50% in mass), before reaching saturation at ca. 3 mW. For a 61-layer LB film of PMDI/CdSt, saturation occurred only at 8 mW. The saturation behavior is similar to the one observed for HPDR13 LB films, though in the latter films saturation took place at 2 mW [18]. The difference in saturation power for the three polymers mentioned may be related to the spectral region of absorption of the dyes [19]. HPDR13 has maximum absorbance at 497 nm, PIPDI at 470 nm and PMDI at 465 nm. As the writing laser operates at 532 nm, distinct photoisomerization rates could affect the power dependence of the optically induced birefringence. Other possible causes are the distinct structures and amount of dyes in the polymers, which could explain the differences between PIPDI and HPDR13. However, PMDI has a T_g and amount of dye very close to those of PIPDI. Therefore, the higher laser power to reach saturation in the birefringence for PMDI/CdSt must again be associated with the type of aggregation in this material. As mentioned earlier, the H-type aggregation, only observed in PMDI/CdSt, appears to be more effective in precluding photoisomerization.

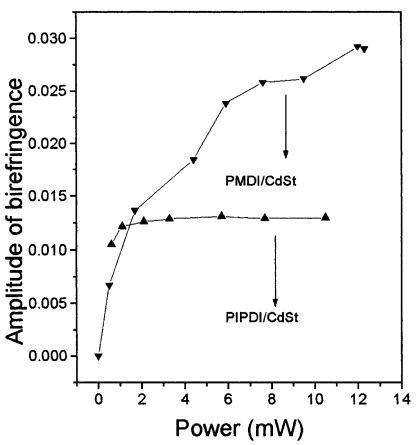

Fig. 9. Amplitude of induced birefringence in the composite LB film of PMDI/CdSt (61-layer), PIPDI/CdSt (61-layer) versus laser power.

In subsidiary experiments with spin-coated films with no CdSt we observed that the maximum induced birefringence is higher for PIPDI ($\Delta n = 0.042$) than for PMDI ($\Delta n = 0.011$). This is consistent with the results for spin-coated films by Meng et al. [20], where the birefringence was higher for an aliphatic polymer, pDR1M (poly[4′-[[2-(methacryloyloxy)-ethyl]ethylamino]-2-chloro-4-nitroazobenzene) than for an aromatic polymer, p-NMNA (poly{4,4′-(1-methylethylidene)bisphenylene 3-{4-4-nitrophenylazo)phenyl]3-azapentadione}. However, the behavior observed for the LB films is opposite (Table 1), which again points to the importance of aggregation in this type of film caused by the interaction with CdSt.

4. Conclusions

The optical storage properties of LB films produced from mixtures of azopolyurethanes and CdSt were affected by aggregation and interaction between the CdSt and the polymer. The H-type aggregation appears to hinder photoisomerization processes in LB films from PMDI/CdSt in comparison with LB films from PIPDI/CdSt and other azopolymers. As a consequence, maximum birefringence was reached at higher laser powers for PMDI/CdSt LB films. Surface pressure and surface potential results for Langmuir monolayers showed that already at the air/water interface, CdSt had a strong effect on the organization of PMDI molecules.

Acknowledgments

This work was supported by FAPESP, CNPq and CAPES (Brazil).

References

[1] Oliveira Jr.ON, Raposo M, Dhanabalan A. Langmuir–Blodgett (LB) and self-assembled polymeric films. In: Nalwa HS, editor. Handbook

surfaces and interfaces of materials. New York: Academic Press; 2001. Chapter 1.
[2] Maack J, Ahuja RC, Mobius D, Tachibana H, Matsumoto M. Thin Solid Films 1994;242:122–6.
[3] Loucif-Saibi R, Nakatani K, Delaire JA, Dumont M, Sekkat Z. Chem Mater 1993;5:229–36.
[4] Bian S, Liu W, Williams J, Samuelson JK, Tripathy SK. Chem Mater 2000;12(6):1585–90.
[5] Itoh M, Harada K, Matsuda H, Ohnishi S, Parfenov A, Tamaoki N, Yatagai T. J Phys D: Appl Phys 1998;31:463–71.
[6] Tripathy SK, Kim D, Li L, Kumar J. Chemtech 1998;28:34–40.
[7] Li XT, Natansohn A, Rochon P. Appl Phys Lett 1999;74:3791–3.
[8] Delaire J, Natani K. Chem Rev 2000;100:1817–45.
[9] Natansohn A, Rochon P. Adv Mater 1999;11:1387–91.
[10] Dos Santos Jr. DS, Mendonça CR, Balogh DT, Dhanabalan A, Cavalli A, Misoguti L, Giacometti JA, Zilio SC, Oliveira Jr. ON. Chem Phys Lett 2000;317:1–5.
[11] Mendonça CR, Dos Santos Jr. DS, Balogh DT, Dhanabalan A, Giacometti JA, Zilio SC, Oliveira Jr. ON. Polymer 2001;42:6539–44.
[12] Dhanabalan A, Dos Santos Jr. DS, Mendonça CR, Misoguti L, Balogh DT, Giacometti JA, Zilio SC, Oliveira Jr. ON. Langmuir 1999;15: 4560–4.
[13] Dos Santos Jr. DS, Mendonça CR, Balogh DT, Giacometti JA, Zilio SC, Oliveira Jr. ON. Synth Met 2001;121(1–3):1479–80.
[14] Kern W. Semicond Int 1984;1:94–5.
[15] Dhanabalan A, Riul Jr. A, Oliveira Jr. ON. Supramol Sci 1998;5(1): 75–81.
[16] Dhanabalan A, Mendonça CR, Balogh DT, Misoguti L, Constantino CJL, Giacometti JA, Zilio SC, Oliveira Jr. ON. Macromolecules 1999; 32:5277–84.
[17] Meng X, Natansohn A, Rochon P. Supramol Sci 1996;3:207–13.
[18] Mendonça CR, Dhanabalan A, Balogh DT, Misoguti L, Dos Santos Jr. DS, Pereira-Da-Silva MA, Giacometti JA, Zilio SC, Oliveira Jr. ON. Macromolecules 1999;32:1493–9.
[19] Xie S, Natansohn A, Rochon P. Macromolecules 1992;5:5531–2.
[20] Meng X, Natansohn A, Rochon P. J Polym Sci, Part B: Polym Phys 1996;34:1461–6.